Rapid Communications

Thresholdless excitation of edge plasmons by transverse current

Aleksandr S. Petrov* and Dmitry Svintsov
Laboratory of 2D Materials' Optoelectronics, Moscow Institute of Physics and Technology, Dolgoprudny 141700, Russia

(Received 24 April 2020; revised 23 July 2020; accepted 23 July 2020; published 1 September 2020)

We theoretically demonstrate that dc electron flow across the junction of two-dimensional electron systems leads to excitation of edge magnetoplasmons. The threshold current for such plasmon excitation does not depend on contact effects and approaches zero for ballistic electron systems, which makes a strong distinction from the well-known Dyakonov-Shur and Cerenkov-type instabilities. We estimate the competing plasmon energy gain from dc current and loss due to electron scattering. We show that plasmon self-excitation is feasible in GaAs-based heterostructures at $T \lesssim 200$ K and magnetic fields $B \lesssim 10$ T.

DOI: 10.1103/PhysRevB.102.121402

Edge plasmon is a collective electronic excitation propagating along the boundary of a two-dimensional electron system (2DES). Since their first observation [1,2], edge plasmons proved to be challenging yet fruitful phenomena to explore. The edge plasmons differ dramatically from their higher-dimensional counterparts: The former usually have longer lifetimes [3,4], manifest extraordinary light confinement [5,6], and exhibit unique chiral properties [7–10] such as unidirectional propagation. These features make edge plasmons promising information carriers in future integrated circuits, but the technological progress is hindered by their laborious excitation. Thus, optical excitation techniques involve ponderous near-field equipment [5] or additional sample processing (e.g., waveguide deployment [3]), whereas electrical excitation of edge plasmons requires ultrashort pulses [11].

In this Rapid Communication, we suggest a simple method for electrical excitation of edge plasmons in continuous regime: Excitation by direct transverse current. This method complements the family of current-driven plasmon instabilities in semiconductor heterostructures containing Cerenkov-type [12,13], beam [14,15], and Dyakonov-Shur [16] instabilities. However, all mentioned cases concern the excitation of 2D plasmons by current copropagating with excited wave. This results either in large threshold velocities for instability onset [13], or in extreme sensitivity to contact effects [17]. Accordingly, though current-driven electromagnetic emission in solids has been observed [18–20], its relation to any plasmon instability is still debated [21–23].

The proposed technique for edge plasmon excitation has no current threshold for sufficiently clean systems and is insensitive to contact effects. It is inherited from a proposal of boundary instability in a 2DES with a fully imaginary (turbulent) spectrum [21,26]. In this Rapid Communication, we show that turbulent plasma instability is the limiting case of a more general phenomenon—instability of edge magnetoplasmons with a well-defined spectrum. We develop a theory of current-driven edge plasmon instabilities, determine their frequencies and growth rates, and suggest a route for their experimental observation.

As an illustrative and exactly solvable model, we study the effect of transverse electric current on interedge magnetoplasmons (IEMPs). These waves exist on the boundary between two conductive half-planes in an external magnetic field B [27–31]. In what follows, we model the boundary as a steplike profile of electron density $n_0(x) = n_l\theta(-x) + n_r\theta(x)$ [32]. IEMP is a chiral mode with the direction of propagation depending on the direction of B and carrier density contrast $n_r - n_l$. For definiteness, we choose $B > 0$, $n_r > n_l$; in this case, the plasmon travels codirectional with the y axis in Fig. 1(a).

The spectrum of IEMPs is nontrivial: In weak fields its frequency is proportional to the magnetic field, while in strong fields the frequency acquires $\ln(\omega_c/\omega_{2d})/\omega_c$ dependence [Fig. 1(b)], where ω_c is the cyclotron frequency and ω_{2D} is the plasma frequency of unbounded 2DES. The dependence of wave damping on carrier momentum relaxation time τ_p is also noteworthy: In weak fields, the IEMP damping rate is two times higher than the usual $1/2\tau_p$ estimate for 2D and 3D plasmons, while in strong fields the damping rate is much lower and scales as $1/B$ [Fig. 1(c)].

In what follows, we demonstrate that IEMPs can be excited by the transverse electric current, and establish the general features of such an instability. In our analysis we adopt the hydrodynamic model for electron transport [33]. In linearized form with respect to variations of carrier density n and drift velocity $\mathbf{u}$, the hydrodynamic equations read

$$\partial_t n + \nabla(n_0\mathbf{u} + \mathbf{u}_0 n) = 0; \tag{1}$$

$$\partial_t \mathbf{u} + (\mathbf{u}_0, \nabla)\mathbf{u} + (\mathbf{u}, \nabla)\mathbf{u}_0 = -\frac{e}{mc}\mathbf{u} \times \mathbf{B} - \frac{e\mathbf{E}}{m}, \tag{2}$$

where $e > 0$ is the elementary charge, m is carrier effective mass, c is the speed of light, $u_0 = u_l\theta(-x) + u_r\theta(x)$ is transverse drift velocity [34], and $\mathbf{E} = -\nabla\varphi$ is plasmon electric field. To find the eigenfrequencies of plasmons, one supplements these equations with self-consistent field relation

*aleksandr.petrov@phystech.edu

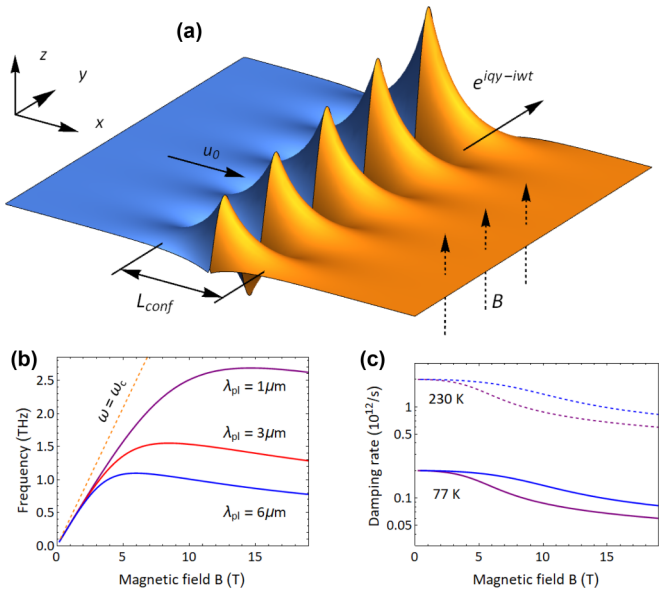

FIG. 1. (a) Schematic of electric potential distribution for an interedge magnetoplasmon confined between two conductive half-planes with characteristic confinement length $L_{\rm conf}$. The plasmon is chiral and propagates with wave vector $q > 0$ if $n_r > n_l$ in magnetic field $B_z > 0$. The growing wave amplitude illustrates the gain from dc current $\mathbf{u}_0$. (b) IEMP spectrum for a GaAs/AlGaAs heterostructure ($m = 0.067m_e$, dielectric permittivity $\varepsilon = 1$ for simplicity) at different plasmon wavelengths $\lambda_{\rm pl} = 2\pi/q \simeq L_{\rm conf}/2$. Carrier densities are $n_l = 10^{11}$ cm^{-2}, $n_r = 9\times10^{11}$ cm^{-2}. Orange dashed line stands for cyclotron frequency. (c) Damping rate dependence from magnetic field for IEMPs from panel (b) at different temperatures; effective momentum relaxation times were assumed to be 0.5 ps for 230 K and 5 ps for 77 K [24,25]. Line colors correspond to plasmon wavelengths defined in panel (b).

$\varphi(x) = -e\mathcal{G}[n] \equiv -e\int d\mathbf{r}' G(\mathbf{r},\mathbf{r}')n(\mathbf{r}')$, where $G(\mathbf{r},\mathbf{r}')$ is the Green's function of Poisson's equation.

The presence of carrier drift makes the conductivity tensor nonlocal in each of the half-planes, which significantly tangles the solution of the resulting eigenvalue problem (see, for example, [35,36]). Fortunately, analytical treatment is greatly simplified if we consider carrier drift as a small perturbation over the IEMP profile in an unbiased 2DES. This is done in the framework of a recently developed perturbation theory for hydrodynamic plasmons [37].

This theory relies on an operator representation of Eqs. (1) and (2). It states that if a plasmon mode with frequency ω is subject to a small perturbation $\hat{V}$, then the perturbation-induced correction to the frequency is given by

$$\delta\omega = \frac{\langle\mathbf{\Phi}|\hat{H}\hat{V}\mathbf{\Phi}\rangle}{\langle\mathbf{\Phi}|\hat{H}\mathbf{\Phi}\rangle}, \tag{3}$$

where $\hat{H}$ is the "'Hamiltonian operator" governing the net energy of the wave. In the particular case of IEMP,

$$\hat{H} = \begin{pmatrix} e^2/m\,\mathcal{G}[\cdot] & 0 & 0 \\ 0 & n_0(x) & 0 \\ 0 & 0 & n_0(x) \end{pmatrix}, \tag{4}$$

and the effect of current is described by the perturbation operator

$$\hat{V} = -i\begin{pmatrix} \partial_x[u_0(x)\cdot] & 0 & 0 \\ 0 & \partial_x[u_0(x)\cdot] & 0 \\ 0 & 0 & u_0(x)\partial_x\cdot \end{pmatrix}, \tag{5}$$

$\mathbf{\Phi} = \{\tilde{n}, \tilde{u}_x, \tilde{u}_y\}^{\rm T}$ is a three-dimensional vector comprising Fourier components of the unperturbed plasmon carrier density and velocity (we denote $\tilde{n} = n_{q,\omega}$), the usage of the dot in operators (4) and (5) is best understood through the example

$$\hat{V}\mathbf{\Phi} = -i\{\partial_x(u_0\tilde{n}),\, \partial_x(u_0\tilde{u}_x),\, u_0\partial_x\tilde{u}_y\}^{\rm T},$$

and the inner product is defined as

$$\langle\Phi|\hat{H}\Phi\rangle = \int d\mathbf{r}\left(\frac{e^2}{m}\tilde{n}^*\mathcal{G}[\tilde{n}] + n_0\tilde{\mathbf{u}}^*\tilde{\mathbf{u}}\right).$$

We managed to evaluate the current-induced perturbation (3) of plasmon frequency for IEMPs in general form [Eq. (A2) in the Appendix], which simplifies for the steplike background density profile:

$$\delta\omega = -ij_0\frac{\left(\frac{m|\tilde{u}_x|^2}{2} - \frac{e^2\tilde{E}_x^2}{2m\omega^2}\right)\Big|_{-0}^{+0}}{\int_{-\infty}^{\infty}[mn_0(|\tilde{u}_x|^2 + |\tilde{u}_y|^2) - e\tilde{\varphi}\tilde{n}]dx}, \tag{6}$$

where the notation $(\cdots)|_{-0}^{+0}$ stands for discontinuity of the quantity across the interface, and $j_0 = n_l u_l = n_r u_r$ is carrier flux.

The correction to plasmon frequency (6) is purely imaginary, which corresponds to wave self-excitation for $\mathrm{Im}\,\delta\omega > 0$, and damping for $\mathrm{Im}\,\delta\omega < 0$. It depends linearly on current j_0 which is a natural consequence of perturbation theory. From the above equation we readily reveal the necessary conditions for edge plasmon excitation by direct current. First, plasmons cannot be excited in the absence of magnetic field; the latter tangles the u_x velocity component with perpendicular electric field E_y leading to a nonzero numerator. Highly symmetrical modes are insensitive to drift as well. The example of such a mode is the proximity plasmon bound between homogeneous 2DES and a metallic electrode [38,39].

To judge on the definite effect of drift, we plug the known distributions of fields in the IEMP mode [28] into Eq. (3) and numerically evaluate the integrals [40]. As a result, we obtain the IEMP growth rate dependence on the cyclotron frequency shown in Fig. 2.

We observe that the instability benefits from pronounced density contrast at the boundary (see the blue arrow in Fig. 2), and its behavior drastically differs in limits of weak and strong magnetic fields. In weak fields the instability growth rate scales linearly with the wave vector and is independent of B. In strong fields, the plasmon growth rate scales as B^2 and is independent of the wave vector. The growth rates in these limiting cases are given by

$$\delta\omega_w \simeq iqj_0\frac{n_r - n_l}{2n_r n_l} \propto \omega_c^0 q^1 \Delta n^1; \tag{7}$$

$$\delta\omega_s \simeq -iqj_0\frac{\omega_c}{\omega}\frac{(n_r - n_l)^2(n_r + n_l)}{8n_r^2 n_l^2} \propto \omega_c^2 q^0 \Delta n^1, \tag{8}$$

where $\omega_c = eB/mc$ is the cyclotron frequency.

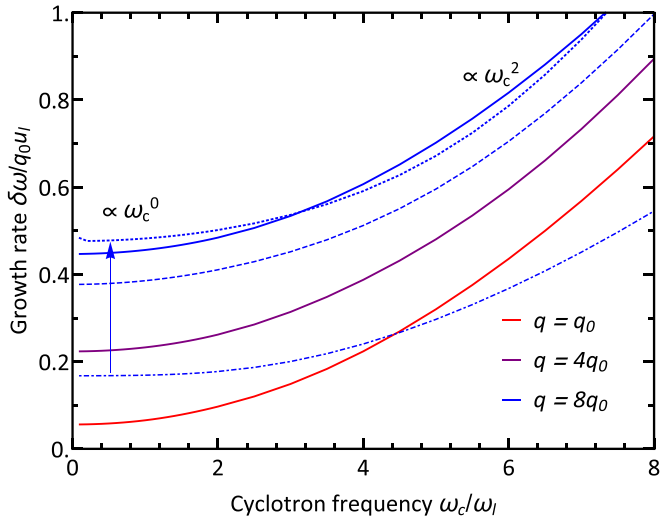

FIG. 2. Calculated IEMP growth rate (in units of q_0u_l) vs cyclotron frequency [normalized by plasma frequency in the left half-plane $\omega_l(q_0)$] at various wave vectors and density contrasts for GaAs/AlGaAs heterostructure, $q_0 = 2\pi/(0.5\ \mu\text{m})$, $u_l = 10^7$ cm/s. Solid lines correspond to relative density contrast $(n_r - n_l)/(n_r + n_l)$ value 0.8, dot-dashed to 0.2, dashed to 0.6, and dotted to 0.9, while n_l is fixed at 10^{11} cm^{-2}. The growth rate in weak fields saturates as the relative density contrast approaches 1 (blue arrow).

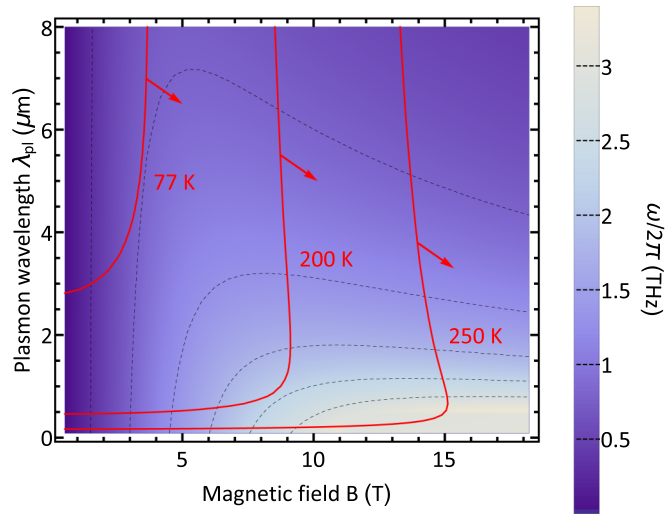

FIG. 3. Color map of edge magnetoplasmon dispersion $\omega_{\text{emp}}(\lambda_{\text{pl}}, B)$ overlaid with "critical lines" of instability calculated at three different temperatures for GaAs/AlGaAs heterostructure. Waves with parameters to the right from critical lines have threshold carrier velocity below the saturation velocity in GaAs ($\sim 2\times10^7$ cm/s). Structural parameters are the same as in Fig. 1(b); effective momentum scattering times are the following: 5 ps for 77 K, 0.75 ps for 200 K, and 0.25 ps for 250 K.

The instability has zero threshold current in the absence of momentum relaxation pathways. In realistic systems, it is mainly hampered by carrier scattering on phonons or impurities. Thus, it is important to estimate the threshold drift velocity u_{th} at which gain (6) takes over scattering loss.

To provide a quantitative picture, we examine the stability of dc current in the GaAs/AlGaAs heterostructure for a wide range of magnetic fields and wavelengths. In Fig. 3, we plot the boundaries separating stability and instability regions at three temperatures; the instability regions are indicated by red arrows. The boundary lines are calculated from the balance between the damping rate at a given wavelength and magnetic field, and the growth rate at GaAs saturation velocity ($\sim 2\times10^7$ cm/s) [41]. We observe that IEMP can be easily excited at 77 K; its excitation at higher temperatures is possible for shorter wavelengths and/or stronger magnetic fields. However, it is not the absolute value of the magnetic field that governs the instability growth rate; instead, it is the ratio of cyclotron and plasma frequencies. Hence, in order to achieve pronounced growth rates one can not only increase the field, but also decrease ω_{2d} (e.g., by depletion of carrier density). For example, electron gas on a surface of liquid helium usually exhibits $\omega_c/\omega_{2d} \simeq 1000$ even at $B = 1$ T [2], which enormously boosts the quadratically scaled growth rate (8).

Another loss mechanism is caused by viscosity, which is extremely challenging to incorporate in exact analysis of edge plasmons [35]. Still, we can roughly estimate the corresponding damping rate as

$$\text{Im}\,\delta\omega_{\text{visc}} \approx -\frac{\nu q^2}{2}, \tag{9}$$

where $\nu = v_F^2\tau_{ee}/4$ is kinematic viscosity; at 77 K and $q = 2\pi/(2\ \mu\text{m})$ we can estimate $\nu \approx 170$ cm^2/s [42–44] and $\text{Im}\delta\omega_{\text{visc}} = -10^{11}$ s^{-1}. The damping rate (9) is several times smaller than the loss from momentum scattering in weak magnetic fields [Fig. 1(c)] and does not affect the results of Fig. 3 much. Still, its role increases at larger wave vectors.

We note that our analysis relies on a hydrodynamic model of electron transport and thus cannot be extended to cover the quantum Hall regime. Still, we can speculate that the instability would be nearly absent in this regime. Indeed, in quantizing magnetic fields the drifting electrons would be bound to skipping orbits and thus would not be able to deliver energy to the edge mode. Still, quantum effects do not affect numerical estimates of Fig. 3 as the necessary condition for their observation $\hbar\omega_c \gg kT$ does not hold for our temperature range.

We stress that edge plasmon instability should be distinguished from the Dyakonov-Shur instability. The latter relies on the surplus of energy gained by plasmon at source over the energy lost at the drain, thus being extremely sensitive to boundary conditions [45]. In contrast, edge plasmon instability is independent of contact effects, as the required energy transfer from dc current to plasmon occurs in the interior of the 2DES in the vicinity of the density step. What is more, the frequency of the excited plasmon is independent of sample length or width provided they significantly exceed plasmon wavelength. These features make IEMP instability a prominent candidate for the creation of resonant-tunable arrays of plasmonic THz emitters.

The proposed technique necessarily requires that the edge mode be localized between two conducting materials so that the electric current could pass through. For instance, modes

such as metal-dielectric interedge plasmon [46] or transverse magnetosound [47] do not satisfy this condition.

It is remarkable that current-induced frequency shift given by Eq. (6) can be obtained purely from energy conservation considerations (see Appendix), similarly to the Reynolds-Orr energy equation known in the fluid turbulence theory [48,49]. However, the strong inhomogeneity of dc current flow ($\partial u_{0x}/\partial y \neq 0$) necessary for turbulence onset in fluids is not required for edge plasmon instability due to nonzero compressibility of the electron system.

Remarkably, edge plasmon instability is just one of numerous manifestations of the flux-to-perturbation energy transfer in plasmonics. For example, it can be used to excite chiral plasmons without magnetic field [9], intersurface magnetoplasmons (3D analog of IEMPs), higher-order (quadrupole, etc.) magnetoplasmon modes bound to a smooth edge [50], or increase the lifetime of decaying modes such as the upper mode of IEMP [28]. It would be of particular interest to examine the stability of proximity magnetoplasmons [38,39] with respect to external source-drain bias due to the relatively simple experimental setup (no need for density contrast). Essentially, the magnetic field will be needed to break the proximity mode symmetry and make it susceptible to drift.

In conclusion, we predicted thresholdless current-driven edge plasmon instability. Possible applications include electrical excitation of edge plasmons in continuous regime and the creation of competitive resonant THz sources. The underlying mechanism for the reported instability is flow-to-perturbation energy transfer that proves to be a general phenomenon in plasmonics and has many potential manifestations.

The authors are grateful to V. Muravev, M. Dyakonov, I. Zagorodnev, and G. Alymov for fruitful discussions and comments. The authors acknowledge support from Russian Foundation for Basic Research, Project No. 18-37-00206, and Foundation for the Advancement of Theoretical Physics and Mathematics BASIS, Project No. 18-1-5-66-1 (development of perturbation theory for edge plasmons). Analysis of instability threshold was supported by Grant No. 18-72-00234 of the Russian Science Foundation.

APPENDIX: FLOW-TO-PERTURBATION ENERGY TRANSFER

We multiply the Euler equation (2) with $n_0\mathbf{u}$, integrate over the whole 2DES, and eliminate the boundary contributions by the Gauss-Ostrogradsky formula that can be done exceptionally by virtue of the localized nature of edge plasmons. Thus, we obtain the following equation for energy balance:

$$\partial_t \int (K+\Pi)dS = \int \frac{e(\mathbf{E},\mathbf{u}_0)}{m} n\, dS - \int n_0\mathbf{u}[(\mathbf{u}_0,\nabla)\mathbf{u} + (\mathbf{u},\nabla)\mathbf{u}_0]dS, \tag{A1}$$

where

$$K+\Pi = \frac{n_0\mathbf{u}^2}{2} - \frac{en\varphi}{2m}$$

is total plasmon energy density. Hence, plasmon energy density changes in time due to its interaction with stationary flow (right-hand side). We stress that electron compressibility is crucial for plasmon excitation; otherwise, the right-hand side of Eq. (A1) vanishes for flows $\partial_i v_{0j} = 0, i \neq j$.

Remarkably, the perturbation theory result (6) can be obtained from Eq. (A1). To do this, we represent all the IEMP characteristics (variations of carrier density, velocity, etc.) in the form $a = \tilde{a}\exp^{-i\omega t - i\delta\omega t + iqy} + \text{c.c.}$, where a is one of the variations, and $\delta\omega \propto u_0$ is the drift-induced correction. Next, we perform time averaging over period $T \gg 2\pi/\omega$ and to the first order of $\mathbf{u}_0$ we obtain

$$\delta\omega = -i\frac{\int_{-\infty}^{\infty} n_0\tilde{v}_x^*\partial_x(u_0\tilde{v}_x)\,dx + \int_{-\infty}^{\infty} n_0\tilde{v}_y u_0\partial_x(\tilde{v}_y)\,dx - e/m\int_{-\infty}^{\infty}\tilde{\varphi}\partial_x(u_0\tilde{n})\,dx}{2\int_{-\infty}^{\infty}(n_0\tilde{\mathbf{u}}^2/2 - e\tilde{n}\tilde{\varphi}/2m)\,dx}, \tag{A2}$$

where we used the following properties of unperturbed IEMP: $\tilde{\varphi}, \tilde{n}, \tilde{v}_y$ are real, $\tilde{v}_x$ is imaginary; dependence of these quantities on drift velocity leads to higher-order terms that we neglect.

Equation (A2) can be also obtained from the perturbation theory and in the case of a steplike background density profile leads to Eq. (3): The first integral in (A2) equals $j_0|\tilde{v}_x|^2/2|_{-0}^{+0}$, the second one is zero, and the last one is equal to $e^2\tilde{E}_x^2/2m\omega^2|_{-0}^{+0}$, which leads us to Eq. (6).

We stress that the result (A2) is more general than illustrative formula (6) as it allows one to calculate the drift-induced correction to the spectrum of a plasmon with an arbitrary profile. In particular, Eq. (A2) covers the case of smooth background carrier profiles, in which higher-order modes (quadrupole, etc.) emerge, and predicts thresholdless instabilities for each of them [if for some profile expression (A2) is negative, one shall simply reverse the dc current flow to switch from decay to instability].

[1] D. B. Mast, A. J. Dahm, and A. L. Fetter, Observation of Bulk and Edge Magnetoplasmons in a Two-Dimensional Electron Fluid, Phys. Rev. Lett. **54**, 1706 (1985).

[2] D. C. Glattli, E. Y. Andrei, G. Deville, J. Poitrenaud, and F. I. B. Williams, Dynamical Hall Effect in a Two-Dimensional Classical Plasma, Phys. Rev. Lett. **54**, 1710 (1985).

[3] V. M. Murav'ev, I. V. Kukushkin, A. Parakhonskiĭ, J. Smet, and K. Von Klitzing, Measurement of the mean free path of edge magnetoplasmons revealed in the spectra of magnetic oscillations of photovoltage in a two-dimensional electron system under microwave radiation, JETP Lett. **83**, 246 (2006).

[4] P. J. M. Peters, M. J. Lea, A. M. L. Janssen, A. O. Stone, W. P. N. M. Jacobs, P. Fozooni, and R. W. van der Heijden, Observation of Audio-Frequency Edge Magnetoplasmons in the Classical Two-Dimensional Electron Gas, Phys. Rev. Lett. **67**, 2199 (1991).

[5] Z. Fei, M. Goldflam, J.-S. Wu, S. Dai, M. Wagner, A. McLeod, M. Liu, K. Post, S. Zhu, G. Janssen *et al.*, Edge and surface plasmons in graphene nanoribbons, Nano Lett. **15**, 8271 (2015).

[6] I. V. Andreev, V. M. Muravev, V. N. Belyanin, and I. V. Kukushkin, Azbel'-kaner-like cyclotron resonance in a two-dimensional electron system, Phys. Rev. B **96**, 161405(R) (2017).

[7] A. C. Mahoney, J. I. Colless, L. Peeters, S. J. Pauka, E. J. Fox, X. Kou, L. Pan, K. L. Wang, D. Goldhaber-Gordon, and D. J. Reilly, Zero-field edge plasmons in a magnetic topological insulator, Nat. Commun. **8**, 1836 (2017).

[8] D. Jin, T. Christensen, M. Soljačić, N. X. Fang, L. Lu, and X. Zhang, Infrared Topological Plasmons in Graphene, Phys. Rev. Lett. **118**, 245301 (2017).

[9] J. C. Song and M. S. Rudner, Chiral plasmons without magnetic field, Proc. Natl. Acad. Sci. USA **113**, 4658 (2016).

[10] V. M. Muravev, A. A. Fortunatov, I. V. Kukushkin, J. H. Smet, W. Dietsche, and K. von Klitzing, Tunable Plasmonic Crystals for Edge Magnetoplasmons of A Two-Dimensional Electron System, Phys. Rev. Lett. **101**, 216801 (2008).

[11] G. Ernst, R. J. Haug, J. Kuhl, K. von Klitzing, and K. Eberl, Acoustic Edge Modes of the Degenerate Two-Dimensional Electron Gas Studied by Time-Resolved Magnetotransport Measurements, Phys. Rev. Lett. **77**, 4245 (1996).

[12] M. Krasheninnikov and A. Chaplik, Instabilities of two-dimensional plasma waves, Sov. Phys. JETP **52**, 279 (1980).

[13] S. A. Mikhailov, Plasma instability and amplification of electromagnetic waves in low-dimensional electron systems, Phys. Rev. B **58**, 1517 (1998).

[14] K. Kempa, P. Bakshi, J. Cen, and H. Xie, Spontaneous generation of plasmons by ballistic electrons, Phys. Rev. B **43**, 9273 (1991).

[15] V. Gruzinskis, R. Mickevičius, J. Pozela, and A. Reklaitis, Collective electron interaction in double-barrier GaAs structures, Europhys. Lett. **5**, 339 (1988).

[16] M. Dyakonov and M. Shur, Shallow Water Analogy for a Ballistic Field Effect Transistor: New Mechanism of Plasma Wave Generation by dc Current, Phys. Rev. Lett. **71**, 2465 (1993).

[17] F. J. Crowne, Contact boundary conditions and the Dyakonov–Shur instability in high electron mobility transistors, J. Appl. Phys. **82**, 1242 (1997).

[18] V. Kopylov and S. Yanchenko, Investigation of the period-doubling bifurcation cascade occurring during the development of magnetohydrodynamic instability in bismuth, Sov. Phys. JETP **65**, 1210 (1987).

[19] A. El Fatimy, N. Dyakonova, Y. Meziani, T. Otsuji, W. Knap, S. Vandenbrouk, K. Madjour, D. Theron, C. Gaquiere, M. Poisson *et al.*, AlGaN/GaN high electron mobility transistors as a voltage-tunable room temperature terahertz sources, J. Appl. Phys. **107**, 024504 (2010).

[20] D. Tsui, E. Gornik, and R. Logan, Far infrared emission from plasma oscillations of Si inversion layers, Solid State Commun. **35**, 875 (1980).

[21] M. Dyakonov, Boundary instability of a two-dimensional electron fluid, Semiconductors **42**, 984 (2008).

[22] A. Chaplik, Absorption and emission of electromagnetic waves by two-dimensional plasmons, Surf. Sci. Rep. **5**, 289 (1985).

[23] C. B. Mendl, M. Polini, and A. Lucas, Coherent terahertz radiation from a nonlinear oscillator of viscous electrons, arXiv:1909.11093.

[24] D. G. Schlom and L. N. Pfeiffer, Upward mobility rocks!, Nat. Mater. **9**, 881 (2010).

[25] I. Andreev, V. Muravev, V. Belyanin, and I. Kukushkin, Measurement of cyclotron resonance relaxation time in the two-dimensional electron system, Appl. Phys. Lett. **105**, 202106 (2014).

[26] A. S. Petrov, D. Svintsov, M. Rudenko, V. Ryzhii, and M. Shur, Plasma instability of 2D electrons in a field effect transistor with a partly gated channel, Int. J. High Speed Electron. Syst. **25**, 1640015 (2016).

[27] V. Volkov and S. A. Mikhailov, Edge magnetoplasmons: Low frequency weakly damped excitations in inhomogeneous two-dimensional electron systems, Sov. Phys. JETP **67**, 1639 (1988).

[28] S. A. Mikhailov and V. Volkov, Inter-edge magnetoplasmons in inhomogeneous two-dimensional electron systems, J. Phys.: Condens. Matter **4**, 6523 (1992).

[29] O. Kirichek and I. Berkutov, Magnetoplasmons in surface electron system on helium at border between regions with different charge density, Low Temp. Phys. **21**, 394 (1995).

[30] P. K. H. Sommerfeld, P. P. Steijaert, P. J. M. Peters, and R. W. van der Heijden, Magnetoplasmons at Boundaries between Two-Dimensional Electron Systems, Phys. Rev. Lett. **74**, 2559 (1995).

[31] G. Sukhodub, F. Hohls, and R. J. Haug, Observation of an Interedge Magnetoplasmon Mode in a Degenerate Two-Dimensional Electron Gas, Phys. Rev. Lett. **93**, 196801 (2004).

[32] It is a usual approximation in edge plasmon studies that holds when the intermediary region is much smaller than plasmon wavelength. That is practically always the case: λ_{pl} is not less than hundreds of nanometers, whereas the size of the intermediary region can be angstrom controlled [51] .

[33] Hydrodynamics provides the simplest framework for a description of plasmons [52].This model can be strictly derived from a kinetic equation if the wave frequency is well below the carrier-carrier collision frequency [53,54]. Electron-phonon and electron-impurity collisions can also result in strong relaxation of nonhydrodynamic harmonics of distribution function, thereby effectively leading to hydrodynamic transport [43].

[34] Generally speaking, the drift velocity is affected by the magnetic field and should have a nonzero y component. In the main text we treat the case when the (remote) y boundaries of the sample have already accumulated a compensatory charge such that the velocity is directed solely along the x axis. In contrast to the 3D case, this compensatory charge spreads over the whole sample [55] and changes the equilbrium charge distribution. However, in wide samples with ordinary doping this effect plays a minor role and vanishes in Corbino geometry .

[35] R. Cohen and M. Goldstein, Hall and dissipative viscosity effects on edge magnetoplasmons, Phys. Rev. B **98**, 235103 (2018).

[36] D. Margetis, M. Maier, T. Stauber, T. Low, and M. Luskin, Nonretarded edge plasmon-polaritons in anisotropic two-dimensional materials, J. Phys. A: Math. Theor. **53**, 055201 (2020).

[37] A. S. Petrov and D. Svintsov, Perturbation theory for two-dimensional hydrodynamic plasmons, Phys. Rev. B **99**, 195437 (2019).

[38] V. M. Muravev, P. A. Gusikhin, A. M. Zarezin, I. V. Andreev, S. I. Gubarev, and I. V. Kukushkin, Two-dimensional plasmon induced by metal proximity, Phys. Rev. B **99**, 241406(R) (2019).

[39] A. A. Zabolotnykh and V. A. Volkov, Interaction of gated and ungated plasmons in two-dimensional electron systems, Phys. Rev. B **99**, 165304 (2019).

[40] See Supplemental Material at http://link.aps.org/supplemental/10.1103/PhysRevB.102.121402 for the mathematical tricks that are needed to evaluate the correction to plasmon frequency (6) and the derivation of Eqs. (7) and (8).

[41] Strictly speaking, Fig. 3 does not take into account the mutual drift-damping influence: The growth rate was calculated on the basis of a collisionless unperturbed state ($\tau_p = \infty$), while the damping rate was taken from the unbiased state [$u_l = u_r = 0$; see Fig. 1(c)]. This may affect the regions where momentum loss is most crucial: Re$\omega \ll$ Imω; in Fig. 3 it corresponds to $B \lesssim 1$ T.

[42] L. Zheng and S. Das Sarma, Coulomb scattering lifetime of a two-dimensional electron gas, Phys. Rev. B **53**, 9964 (1996).

[43] P. S. Alekseev, Negative Magnetoresistance in Viscous Flow of Two-Dimensional Electrons, Phys. Rev. Lett. **117**, 166601 (2016).

[44] A. D. Levin, G. M. Gusev, E. V. Levinson, Z. D. Kvon, and A. K. Bakarov, Vorticity-induced negative nonlocal resistance in a viscous two-dimensional electron system, Phys. Rev. B **97**, 245308 (2018).

[45] M. Cheremisin and G. Samsonidze, D'yakonov-shur instability in a ballistic field-effect transistor with a spatially nonuniform channel, Semiconductors **33**, 578 (1999).

[46] D. R. Mason, S. G. Menabde, S. Yu, and N. Park, Plasmonic excitations of 1D metal-dielectric interfaces in 2D systems: 1D surface plasmon polaritons, Sci. Rep. **4**, 4536 (2015).

[47] P. S. Alekseev and A. P. Alekseeva, Transverse Magnetosonic Waves and Viscoelastic Resonance in a Two-Dimensional Highly Viscous Electron Fluid, Phys. Rev. Lett. **123**, 236801 (2019).

[48] O. Reynolds, IV. On the dynamical theory of incompressible viscous fluids and the determination of the criterion, Philos. Trans. R. Soc. London A **186**, 123 (1895).

[49] W. M. Orr, The stability or instability of the steady motions of a perfect liquid and of a viscous liquid. part II: A viscous liquid, in *Proceedings of the Royal Irish Academy. Section A: Mathematical and Physical Sciences* (JSTOR, Dublin, 1907), Vol. 27, pp. 69–138.

[50] I. L. Aleiner and L. I. Glazman, Novel Edge Excitations of Two-Dimensional Electron Liquid in a Magnetic Field, Phys. Rev. Lett. **72**, 2935 (1994).

[51] W. Kang, H. Stormer, L. Pfeiffer, K. Baldwin, and K. West, Tunnelling between the edges of two lateral quantum Hall systems, Nature (London) **403**, 59 (2000).

[52] A. L. Fetter, Edge magnetoplasmons in a bounded two-dimensional electron fluid, Phys. Rev. B **32**, 7676 (1985).

[53] D. Svintsov, Hydrodynamic-to-ballistic crossover in Dirac materials, Phys. Rev. B **97**, 121405(R) (2018).

[54] P. L. Bhatnagar, E. P. Gross, and M. Krook, A model for collision processes in gases. I. Small amplitude processes in charged and neutral one-component systems, Phys. Rev. **94**, 511 (1954).

[55] A. Shik, Edge charges and the Hall effect in semiconductors, J. Phys.: Condens. Matter **5**, 8963 (1993).